Automatic Generation of Differential-Input Differential-Output Second-Order Filters Based on a Differential Pair

Brent J. Maundy, Ahmed S. Elwakil, and Leonid Belostotski

***Abstract*—In this paper, the generation of differential-input differential-output second-order active filters based on a common-source differential amplifier is systematically conducted using two-port network modeling techniques which enable exploiting the power of symbolic math CAD tools. Starting from a generic two-transistor differential-pair structure, and the maximum possible number of surrounding impedances, all possible filters are derived and classified. In particular, 35 transfer functions and a total of 876 filters are found to be possible. Due to employing a 2×2 transmission matrix representation of each transistor, flexibility in examining parasitic effects on the derived transfer functions is achieved and can be easily automated within the design framework. Selected filters are constructed and experimentally verified using discrete transistors. The operation of some filters is also verified with simulations using a 65-nm CMOS process.**

***Index Terms*—Circuit theory, CMOS, filter theory, *RLC* active filters, symbolic math.**

I. Introduction

FILTERS, from their birth as part of circuit theory and later as filter theory, have been an indispensable part of circuits and systems [1]. Although, filter theory as a discipline in its own right is a mature field, there are still contributions being made to the area either on the structural level, such as in log-domain filters [2], [3] or in realization via employing new analog circuit building blocks, such as the current conveyor and its many variants [4]–[6] or MEMs devices for very high frequency applications [7]. Differential filter design is well known and has been particularly approached using Gm-C or Switched-C structures [8], [9]. These filters have a wide range of applications particularly in bio-medicine [10]–[12]. Automating the synthesis of analog circuits has always been approached using custom algorithms that are dependent on predefined blocks [13]–[15]. For example, an operational amplifier, is assumed to be the active device and hence the synthesis algorithm is customized to this particular device's parameters or customized to a certain topology [15], [16]. Contributions in the case of active filter design (see [17] and the references therein) mainly use numerical optimization techniques to refine the design of a specific given filter structure. However, most recently, the authors of this paper have embarked on a research effort that aims at utilizing the nowadays very powerful symbolic mathematics CAD tools in order to systematically design active analog filters independent of any particular device. This effort has resulted in a series of research articles that started with [18] where all possible single-transistor-based filters were identified and classified. This paved the way for employing selected filters in new applications as demonstrated in [19]–[21] with significant improvement in performance that would have not been possible without discovering these filters. In subsequent articles, all possible differential second-order filters that can be based around a two-transistor cross-coupled cell were systematically identified and classified in [22] while two-transistor multifunction filters were reported in [23]. In each of these articles, the concept of two-port network transmission matrix representation of a transistor was combined with the powerful symbolic mathematical tools of Maple[1] [24] to automate the search for all possible valid filters under a prespecified set of constraints that guarantee the proper dc biasing of the transistors and the stability of the filters. The automation process is independent of the actual active block that will be used in realizing the filter since the synthesis procedure is based in the frequency domain on a general two-port network transmission matrix defined by

$$\begin{bmatrix} V_1 \\ I_1 \end{bmatrix} = \begin{bmatrix} a_{11} & a_{12} \\ a_{21} & a_{22} \end{bmatrix} \begin{bmatrix} V_2 \\ -I_2 \end{bmatrix} = [T] \begin{bmatrix} V_2 \\ -I_2 \end{bmatrix} \tag{1}$$

where V_1 and I_1 are the voltage and current at the input ports, while V_2 and I_2 are those at the output port as shown in Fig. 1 [25].

This two-port network representation assumes the device is linearized around its dc operating point. When used to model an MOS transistor for example, different transmission matrices

Manuscript received May 11, 2018; revised October 29, 2018 and January 23, 2019; accepted April 6, 2019. Date of publication April 23, 2019; date of current version May 22, 2020. This work was supported by NSERC under Discovery Grant RGPIN-2014-05653. This paper was recommended by Associate Editor X. Zeng. *(Corresponding author: Brent J. Maundy.)*

B. J. Maundy and L. Belostotski are with the Department of Electrical and Computer Engineering, University of Calgary, Calgary, AB T2N 1N4, Canada (e-mail: bmaundy@ucalgary.ca; lbelosto@ucalgary.ca).

A. S. Elwakil is with the Department of Electrical and Computer Engineering, University of Sharjah, Sharjah, UAE, and also with the Department of Electrical and Computer Engineering, University of Calgary, Calgary, AB T2N 1N4, Canada (e-mail: elwakil@ieee.org).

Digital Object Identifier 10.1109/TCAD.2019.2912933

[1]Maple math software features a powerful engine with an interface that allows a user to analyze, explore, visualize, and solve mathematical problems. For example to solve the three equations $x^2y^2 = 0$, $x - y = 1$, and $x \neq 0$ for x and y requires the command solve ($\{x^2y^2 = 0, x - y = 1, x \neq 0\}$) with solution $\{x = 1, y = 0\}$.

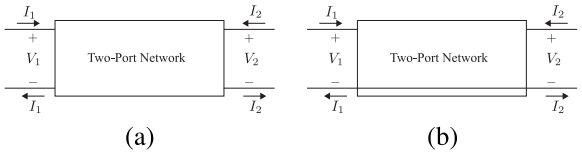

Fig. 1. (a) General two-port network. (b) Common ground two-port network.

can be used depending on the sophistication of the transistor model needed for analysis. Two such matrices are given in (2a)–(2c), namely,

$$[T_1] = \begin{bmatrix} 0 & -\frac{1}{g_m} \\ 0 & 0 \end{bmatrix} \tag{2a}$$

$$[T_2] = \begin{bmatrix} -\frac{1}{g_m r_o} & -\frac{1}{g_m} \\ 0 & 0 \end{bmatrix} \tag{2b}$$

$$[T_3] = \begin{bmatrix} \frac{(1/r_o + sC_{gd})}{sC_{gd} - g_m} & \frac{1}{sC_{gd} - g_m} \\ \frac{(C_{gd}C_{gs}r_o s + C_{gd}g_m r_o + C_{gs} + C_{gd})s}{sC_{gd} - g_m} & \frac{(C_{gs} + C_{gd})s}{sC_{gd} - g_m} \end{bmatrix}. \tag{2c}$$

The simplest model of (2a), considers only an ideal MOS transistor with small-signal transconductance g_m. If the transistor's output resistance r_o must be factored in (as in the case of modern short channel devices) then (2b) can be used. If r_o in addition to the parasitic gate-to-source capacitance C_{gs} and gate-to-drain capacitance C_{gd} are included, then the matrix of (2c) can be used. More complex matrices can be developed depending on the level of complexity in the transistor model. However, in all cases the matrix remains to be a 2×2 matrix. Furthermore, the elements of the matrix can be measured experimentally using a standard network analyzer. If a transistor SPICE model is available, it is easy to perform a sequence of simulations that would yield its two-port network matrix values which can then be fed into MAPLE [26], [27]. The automated search process starts by considering a general architecture where the transistors [modeled first using (2a)] are surrounded by unknown impedances that are exhaustively changed in search for every possible combination that yields a valid second-order filter with the transistors properly biased in the saturation mode. In this paper, we seek to show the massive number of filters (a total of 876) that can be discovered by using this symbolic analysis technique based on MAPLE and two-port network models with the complete code algorithms provided. For that purpose, we select the generalized differential-input differential-output filter structure depicted in Fig. 2(a) formed of a differential amplifier, a biasing tail current I_b, source, and load impedances (Z_s and Z_L) in addition to five other surrounding impedances. Using symbolic analysis, we can: 1) find all possible differential transfer functions from this structure; 2) examine all the possible lowpass (LP), highpass (HP), bandpass (BP), bandstop (BS), gain equalizer (GE), or allpass filters that can be obtained from this topology with the number and type of filters corresponding to each transfer function identified separately; and 3) derive expressions for the differential input and output impedances.

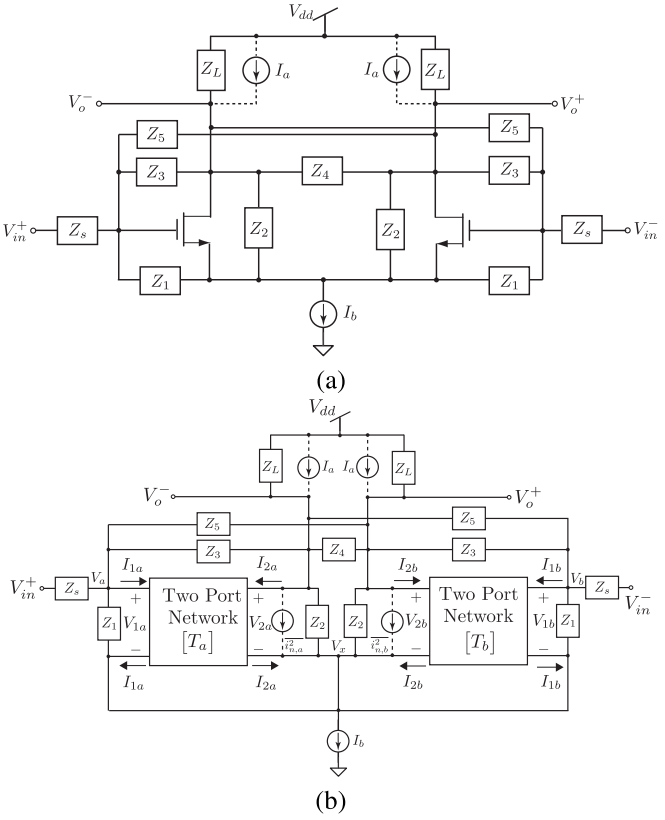

Fig. 2. Proposed differential-input differential-output filter structure (a) circuit based on the differential pair surrounded by passive impedances in a lattice like arrangement and (b) its two port representation to allow for a complete analysis, including thermal noise sources $\overline{i_{n,a}^2}$ and $\overline{i_{n,b}^2}$.

In some of the derived filters, we show that the transfer function remains second-order while in others it changes to third- or even fourth-order when the transistor parasitics are considered. This is easily done by replacing the matrix $[T_1]$ with $[T_3]$ given above in the code. Hence, it allows a designer to quickly check which filters are most susceptible to parasitics, quantize their effects, and arrive to an optimal filter subset on the transfer function level. We further show how to include noise sources into the symbolic analysis to derive the noise figure (NF). It is important to stress that the results obtained here can be easily customized to any active building block with a known transmission matrix and does not apply to transistor-based designs only. It is also important to mention that any mathematical software package with a strong symbolic engine can be used to replace MAPLE.

In Section II, we present the proposed differential generalized topology, its governing equations, and the flowchart of the symbolic generation method. The general transfer function, differential-input impedance, and differential-output impedance expressions are derived using MAPLE as functions of the two-port network parameters. In Section II-A, all possible filters consisting of three or four impedance elements in the general topology are presented, discussed, and contrasted in tables. We restricted our search space to the cases of three or four impedances only since it is well-known that only two capacitors/inductors are required to realize a second-order filter. However, the given codes can easily be run for search

of filters with more impedances in the circuit [see Fig. 2(a)]. For biasing purposes,[2] only impedances that allow each transistor to be properly biased are considered. This step cannot be automated and requires the user to supply MAPLE with all the suitable set of impedances that can be considered, as shown later in Table I. In Section II-B sample filters from the obtained results are designed and compared to confirm the correctness of the search codes. Parasitic effects on sample filters' performance are studied also using symbolic analysis and experimental results using discrete transistors for several circuits are presented in Section III for conclusive verification. Although the symbolic search code targets second-order filters, higher-order filters can be easily obtained by using multiple second-order sections, as demonstrated in Section IV for the case of a forth-order BP filter. Finally, the conclusions are given in Section V.

II. Differential Filter Topology

The differential filter topology under study here is shown in Fig. 2(a) while its two-port network representation is shown in Fig. 2(b). The circuit can be thought of as the common-source differential pair surrounded by the network of impedances $Z_{1\to5}$ along with the load impedances Z_L both in feedforward and feedback arrangements. Impedances $Z_{1,2,3}$ form a π network while sharing Z_2 while impedances $Z_{3,5}$ form a lattice like structure while sharing Z_4. The source impedance Z_s is considered in the structure and optional current sources I_a can be placed around Z_L to ensure that all biasing conditions are met. Neglecting the thermal noise sources, small signal ac analysis in the Laplace domain yields the following set of nodal and mesh equations:

$$0 = I_{1a} + I_{2a} + I_{1b} + I_{2b} + \frac{(V_b - V_x)}{Z_1} + \frac{(V_o^- - V_x)}{Z_2} + \frac{(V_o^+ - V_x)}{Z_2} + \frac{(V_a - V_x)}{Z_1} \tag{3a}$$

$$I_{1a} = \frac{(V_{\text{in}}^+ - V_a)}{Z_s} + \frac{(V_o^- - V_a)}{Z_3} + \frac{(V_x - V_a)}{Z_1} + \frac{(V_o^+ - V_a)}{Z_5} \tag{3b}$$

$$I_{1b} = \frac{(V_{\text{in}}^- - V_b)}{Z_s} + \frac{(V_o^+ - V_b)}{Z_3} + \frac{(V_x - V_b)}{Z_1} + \frac{(V_o^- - V_b)}{Z_5} \tag{3c}$$

$$I_{2a} = \frac{(V_a - V_o^-)}{Z_3} + \frac{(V_x - V_o^-)}{Z_2} + \frac{(0 - V_o^-)}{Z_L} + \frac{(V_o^+ - V_o^-)}{Z_4} + \frac{(V_b - V_o^-)}{Z_5} \tag{3d}$$

$$I_{2b} = \frac{(V_b - V_o^+)}{Z_3} + \frac{(V_x - V_o^+)}{Z_2} + \frac{(0 - V_o^+)}{Z_L} + \frac{(V_o^- - V_o^+)}{Z_4} + \frac{(V_a - V_o^+)}{Z_5} \tag{3e}$$

$$V_o^+ = V_x + V_{2b},\ V_o^- = V_x + V_{2a} \tag{3f}$$

$$V_a = V_x + V_{1a},\ V_b = V_x + V_{1b} \tag{3g}$$

$$V_{1a} = a_{11}V_{2a} - a_{12}I_{2a},\ V_{1b} = b_{11}V_{2b} - b_{12}I_{2b} \tag{3h}$$

$$I_{1a} = a_{21}V_{2a} - a_{22}I_{2a},\ I_{1b} = b_{21}V_{2b} - b_{22}I_{2b} \tag{3i}$$

where $a_{11} \to a_{22}$ (respectively $b_{11} \to b_{22}$) are the four elements of the transmission matrix representing one of the transistors and shown in (3h)–(3i). Note that (3a)–(3c), represent nodal equations written at nodes, V_x, V_a, and V_b, respectively. At the two outputs, the nodal equations are given by (3d) and (3e). Mesh equations are represented by (3f)–(3g). For simplicity, we assume that the two-transistors forming the differential-pair are identical meaning that $[T_a] = [T_b]$ and hence one set of parameters ($a_{11} \to a_{22}$) appears in the subsequent analysis. Equations (3a)–(3i) are solved using Maple in Algorithm 1 and shown in the Appendix to yield a differential transfer function

$$H(s) = -\frac{a_{12}(Z_5 - Z_3) + Z_3Z_5}{Z_\Delta + a_{11}Z_A + a_{12}Z_B + a_{21}Z_C + a_{22}Z_D} \tag{4}$$

where $H(s) = (V_o^+ - V_o^-)/(V_{\text{in}}^+ - V_{\text{in}}^-)$ and

$$Z_\Delta = Z_s(Z_3 - Z_5)(1 + \Delta a) \tag{5a}$$

$$Z_A = Z_3Z_5 + Z_3Z_s + Z_5Z_s + \frac{Z_3Z_5Z_s}{Z_1} \tag{5b}$$

$$Z_B = Z_3 + Z_5 + 4Z_s + \frac{Z_A}{Z_L} + \frac{Z_3Z_5(1 + Z_s)(2Z_2 + Z_4)}{Z_1Z_2Z_4} + Z_s(Z_3 + Z_5)\left(\frac{2}{Z_4} + \frac{1}{Z_2} + \frac{1}{Z_1}\right) \tag{5c}$$

$$Z_C = Z_3Z_5Z_s \tag{5d}$$

$$Z_D = Z_3Z_5Z_s\left(\frac{2}{Z_4} + \frac{1}{Z_2} + \frac{1}{Z_L}\right) + Z_s(Z_3 + Z_5) \tag{5e}$$

and $\Delta a = a_{11}a_{22} - a_{12}a_{21}$. The input and output differential impedances[3] $Z_{\text{in}_d}(s)$ and $Z_{\text{out}_d}(s)$ are likewise obtained in the forms

$$Z_{\text{in}_d}(s) = \frac{2Z_s\left(Z_\Delta + a_{11}Z_A + a_{12}\tilde{Z}_B + a_{21}Z_C + a_{22}Z_D\right)}{Z_\Delta + a_{11}(Z_A - Z_3Z_5) + a_{12}\hat{Z}_B + a_{21}Z_C + a_{22}Z_D} \tag{6}$$

and

$$Z_{\text{out}_d}(s) = \frac{2(a_{12}Z_A + a_{22}Z_C)}{Z_\Delta + a_{11}Z_A + a_{12}Z_B + a_{21}Z_C + a_{22}Z_D} \tag{7}$$

where

$$\tilde{Z}_B = Z_3 + Z_5 + 4Z_s + \frac{Z_s}{Z_1}(Z_3 + Z_5) + Z_A\left(\frac{2}{Z_4} + \frac{1}{Z_2} + \frac{1}{Z_L}\right)$$

$$\hat{Z}_B = 4Z_s + \frac{Z_s}{Z_L}(Z_3 + Z_5) + \frac{Z_C}{Z_1}\left(\frac{2}{Z_4} + \frac{1}{Z_2} + \frac{1}{Z_L}\right) + Z_s(Z_3 + Z_5)\left(\frac{2}{Z_4} + \frac{1}{Z_2} + \frac{1}{Z_1}\right).$$

From (4), (6), and (7) it is possible to compute $H(s)$, $Z_{\text{in}_d}(s)$, and $Z_{\text{out}_d}(s)$ for any impedance combination in addition to

[2]For example, an inductor between the gate and source terminals is not allowed otherwise the device will be off. Likewise an inductor between drain and source is prohibited.

[3]Here, differential impedance refers to the Thevenin's impedance seen at the input and output ports but taken differentially. For example, $Z_{\text{out}_d} = [(V_{\text{th}}^+ - V_{\text{th}}^-)/(I_{\text{th}}^+ - I_{\text{th}}^-)]|_{V_{\text{in}}^+ = V_{\text{in}}^- = 0}$.

TABLE I
TABLE OF POSSIBLE IMPEDANCE COMBINATIONS THAT ALLOW THE TRANSISTORS TO BE BIASED AND THE NUMBER OF IMPEDANCES IN EACH SET

Impedance	Possibilities	No. of Impedances
Z_s	R_s, C_s, L_s	3
$Z_{1,2}$	R_i, C_i, $R_i//C_i$, R_i+C_i, $L_i+C_i (i=1,2)$	5,5
$Z_{3,4,5}$	R_i, C_i, L_i, $R_i//C_i$, R_i+C_i, L_i+C_i, $L_i//C_i (i=3,4,5)$	7,7,7
Z_L	R_L, C_L, L_L, $R_L//C_L$, $L_L//C_L$	5

a given transmission matrix model represented by (2a)–(2c). Note that (4), (6), and (7) are small signal approximations which are valid assuming I_b and $V_{\rm dd}$ are constant at dc values. To determine what filters can be derived from the proposed basic topology, it is necessary to exhaust all possible combinations of the impedances $Z_{s,1,2,\ldots,5,L}$ to report valid sets that result in a second-order transfer function of the form

$$H(s) = K\frac{N_{XY}(s)}{s^2 + \frac{\omega_o}{Q}s + \omega_o^2} \tag{8}$$

where ω_o is the pole frequency, K is the filter gain ($K \in \{K_{\rm LP}, K_{\rm BP}, K_{\rm HP}, K_{\rm BS}, K_{\rm GE}\}$), and Q is the pole quality factor, $N_{XY}(s) \in \{N_{\rm BS}(s), N_{\rm BP}(s), N_{\rm HP}(s), N_{\rm LP}(s), N_{\rm GE}(s)\}$ with $N_{\rm BS}(s) = s^2 + \omega_o^2$, $N_{\rm BP}(s) = (\omega_o/Q)s$, $N_{\rm HP}(s) = s^2$, $N_{\rm LP}(s) = \omega_o^2$, and $N_{\rm GE}(s) = s^2 + (\omega_o/Q_z)s + \omega_o^2$, each representing BS, BP, HP, LP, and GE filters, respectively. For $Q_z = -Q$ an allpass filter is generated. Note that we restrict our results to second-order transfer functions simply because they form the basic building block in higher order filter design [1]. Furthermore, to effectively determine which filters can be derived from the basic topology, it is necessary to establish the impedance combinations that can be allowed across the transistor terminals to ensure proper biasing at all times. The possible list of combinations is given in Table I where the + sign refers to a series connection and the // sign refers to a parallel connection. Only for the case when the load impedances are pure capacitances ($Z_L = 1/sC_L$) will the bias current sources I_a be required [see Fig. 2(a)]. These possible impedance settings are supplied to Maple to perform an exhaustive search as described in Algorithms 1 and 2. The flowchart shown in Fig. 3 is a summary of the automated procedure with Algorithms 2 and 3 in the Appendix used to compute parameters $\omega_o, Q, Q_z, K_{\rm LP}, K_{\rm BP},$ and $K_{\rm HP}$ and the filter type from $K_{\rm LP}, K_{\rm BP},$ and $K_{\rm HP}$, respectively.

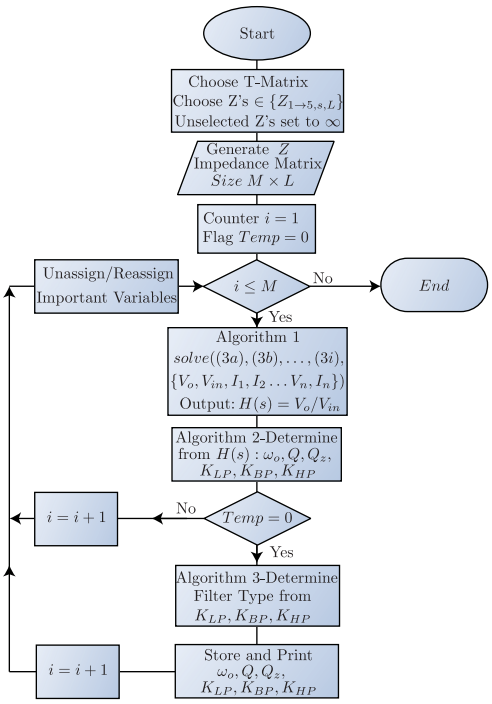

Fig. 3. Simplified flowchart of the generation method to determine all possible differential filters of the type shown in Fig. 2. Note $L = 7$ and M depends on the impedances chosen, 3 or 4 (including Z_s), and the number of possible choices in Table I. For example, if four impedances are chosen such that $Z = [Z_s, Z_1, Z_4, Z_L]$, then $M = 3 \times 5 \times 7 \times 5 = 525$. The remaining impedances $Z_2 = Z_3 = Z_5 = \infty$ or open circuit. Z_s cannot be ∞ or open circuit.

A. Transfer Functions and Possible Filters

Since seven impedances are employed around the basic differential amplifier, a minimum of three impedances combined are necessary to obtain a second-order transfer function consisting of a maximum of two independent parameters. However, if we restrict Z_s to always being a part of that combination having a finite value because the proposed circuit is driven by a differential voltage source which must be present, then straightforward combinational analysis yields ${}_6C_2 = 15$ possible transfer functions. That is, Z_s plus two impedances yields 15 possible transfer functions. If we select three or four impedances out of $Z_{1,2,\ldots,5,L}$ then ${}_6C_3 = 20$, and ${}_6C_4 = 15$. Selecting Z_s plus 4 impedances (${}_6C_4$) evidently makes the filter far from optimal in terms of the component count. Therefore, we present ${}_6C_2 = 15$ and ${}_6C_3 = 20$ possible transfer functions, respectively, for three and four impedance elements since Z_s cannot be ∞ or an open circuit. Using the simplified transistor model of (2a) supplied to Maple [24] and following the flowchart of Fig. 3, the resulting transfer functions and number of possible filters from each transfer function with three and four impedances are shown in Tables II and III, respectively. From Tables II and III, some general observations can be made.

1) Impedance combinations whose transfer functions do not depend on Z_s, examples #7, #9, and #14 of Table II or #15 of Table III, imply that Z_s can be zero. Such filters are derived solely based on combinations of Z_2, Z_4, and Z_L.
2) Impedance combinations having negative signs in the denominator are the result of positive feedback. Such filters have the potential to have large Q's and always involve Z_5. Having negative signs in the denominator also implies the possibility of right hand plane poles and possibly extra conditions need to be satisfied to ensure stability.

TABLE II
LIST OF POSSIBLE THREE IMPEDANCE SETTINGS AND CORRESPONDING TRANSFER FUNCTIONS. THE NUMBER AND TYPE OF POSSIBLE FILTERS FROM EACH TRANSFER FUNCTION ARE ALSO LISTED. A TOTAL OF 115 FILTERS ARE POSSIBLE

Impedances	No	$H(s)$	LP	HP	BP	BS	GE/AP
Z_s, Z_1, Z_2	1	$\frac{g_m Z_1 Z_2}{Z_1+Z_s}$	6	0	2	0	0
Z_s, Z_1, Z_3	2	$\frac{g_m Z_3 - 1}{1+Z_s\left(g_m+\frac{1}{Z_1}\right)}$	2	0	0	1	0
Z_s, Z_1, Z_4	3	$\frac{1}{2}\frac{g_m Z_1 Z_4}{Z_1+Z_s}$	6	0	6	1	0
Z_s, Z_1, Z_5	4	$-\frac{g_m Z_5+1}{Z_s\left(g_m-\frac{1}{Z_1}\right)-1}$	1	0	0	1	0
Z_s, Z_1, Z_L	5	$\frac{g_m Z_1 Z_L}{Z_1+Z_s}$	6	0	6	1	0
Z_s, Z_2, Z_3	6	$\frac{g_m Z_3 - 1}{1+Z_s\left(g_m+\frac{1}{Z_2}\right)+\frac{Z_3}{Z_2}}$	2	0	2	1	2
Z_s, Z_2, Z_4	7	$\frac{g_m Z_2 Z_4}{2Z_2+Z_4}$	0	0	3	2	0
Z_s, Z_2, Z_5	8	$-\frac{g_m Z_5+1}{Z_s\left(g_m-\frac{1}{Z_2}\right)-\frac{Z_5}{Z_2}-1}$	2	0	1	1	2
Z_s, Z_2, Z_L	9	$\frac{g_m Z_2 Z_L}{Z_2+Z_L}$	0	0	3	1	0
Z_s, Z_3, Z_4	10	$\frac{g_m Z_3 - 1}{1+Z_s\left(g_m+\frac{2}{Z_4}\right)+\frac{2Z_3}{Z_4}}$	2	1	5	1	2
Z_s, Z_3, Z_5	11	$-\frac{\left(g_m+\frac{1}{Z_5}-\frac{1}{Z_3}\right)}{g_m Z_s\left(\frac{1}{Z_5}-\frac{1}{Z_3}\right)-\left(\frac{1}{Z_5}+\frac{1}{Z_3}+\frac{4Z_s}{Z_3 Z_5}\right)}$	0	0	0	0	4
Z_s, Z_3, Z_L	12	$\frac{g_m Z_3 - 1}{1+Z_s\left(g_m+\frac{1}{Z_L}\right)+\frac{Z_3}{Z_L}}$	2	1	5	0	2
Z_s, Z_4, Z_5	13	$-\frac{g_m Z_5+1}{Z_s\left(g_m-\frac{2}{Z_4}\right)-\frac{2Z_5}{Z_4}-1}$	2	1	3	1	2
Z_s, Z_4, Z_L	14	$\frac{g_m Z_L Z_4}{2Z_L+Z_4}$	0	0	6	1	0
Z_s, Z_5, Z_L	15	$\frac{g_m Z_5+1}{1+Z_s\left(\frac{1}{Z_L}-g_m\right)+\frac{Z_5}{Z_L}}$	2	1	3	0	2

3) The largest number of possible filters (761) is obtained from the four impedance combinations while the three impedance filters can generate 115 valid filters.
4) Tables II and III, show that allpass filters are possible. However, determination of what allpass filters are possible can only be accomplished by examining on a case by case basis the filters which result in $Q_z = -Q$.
5) While not shown in Tables II or III, some of the reported valid filters have three capacitive or inductive elements. Such filters are nonoptimal in the sense that they use more than the minimum number of reactive elements but were not excluded by our Maple code.

B. Sample Filters and Nonideal Effects

From Tables II and III, there are 876 possible filters that can result from the generalized topology. Of course not all the filters will be optimum in the sense that they contain a minimum number of components or have a straightforward biasing scheme. It is not the subject of this paper to investigate which filters are optimal. However, it will be intuitive to examine a sample of the reported possible filters to illustrate the general observations in Section II-A. For this, we choose some filters from Tables II and III to compare and contrast their gain K, pole frequency ω_o, quality factors Q and Q_z as revealed in Table IV. In Section II-C, input and output impedances of the sample filters will be discussed.

Beginning first with LP1 of Table IV; this three impedance filter taken from Table II is a low Q filter ($Q < 1/2$), with pole frequency independent of g_m and having gain K which can be greater than or less than one. If transmission matrix (2c) is used instead of (2a), a right half plane zero exists at $s_z = (g_m R_3 - 1/R_3 C_{gd})$ and a high frequency left half plane real pole can be observed as well since the a cubic transfer function results in this case. The dc gain is modified to $\widetilde{K} = [(g_m R_3 - 1)/(1 + R_3((1/R_L) + (1/r_o)))]$. In comparison, LP2 of Table IV can have $Q > 1/2$ because of the presence of the negative sign associated with the positive feedback through R_5. However, like LP1 it has its pole frequency independent of g_m and can have a gain which is greater than or less than one. If transmission matrix (2c) is used instead of (2a), this filter will also have a right half plane zero at $s_z = [(g_m R_5 + 1)/(R_5 C_{gd})]$ and a high frequency left half plane real pole. The dc gain of LP2 is modified to $\widetilde{K} = [(g_m R_5 + 1)/(1 + R_5((1/R_L) + (1/r_o)))]$ in this case. Examining HP3 of Table IV, we note again that the pole frequency is independent of g_m. Attempting to achieve gains greater than one however comes at the detriment of widely separated poles making this a low Q filter with $Q < 1/2$. Employing transmission matrix (2c) instead of (2a), a right half plane zero exists at $s_z = [(g_m R_3 - 1)/(R_3 C_{gd})]$ along with a high frequency left half plane real pole. The dc

TABLE III
LIST OF POSSIBLE FOUR IMPEDANCE SETTINGS AND CORRESPONDING TRANSFER FUNCTIONS. THE NUMBER AND TYPE OF FILTERS POSSIBLE FROM EACH TRANSFER FUNCTION ARE ALSO LISTED. A TOTAL OF 761 FILTERS ARE POSSIBLE

Impedances	No	$H(s)$	LP	HP	BP	BS	GE/AP
Z_s, Z_1, Z_2, Z_3	1	$\frac{g_m Z_3 - 1}{1 + Z_s\left(g_m + \frac{1}{Z_1} + \frac{1}{Z_2}\right) + \frac{Z_3}{Z_2}\left(1 + \frac{Z_s}{Z_1}\right)}$	12	0	6	2	0
Z_s, Z_1, Z_2, Z_4	2	$\frac{g_m Z_1 Z_2 Z_4}{(Z_1 + Z_s)(2Z_2 + Z_4)}$	36	2	40	5	0
Z_s, Z_1, Z_2, Z_5	3	$-\frac{g_m Z_5 + 1}{Z_s\left(g_m - \frac{1}{Z_1} - \frac{1}{Z_2}\right) - \frac{Z_5}{Z_2}\left(1 + \frac{Z_s}{Z_1}\right) - 1}$	12	0	6	2	2
Z_s, Z_1, Z_2, Z_L	4	$\frac{g_m Z_1 Z_2 Z_L}{(Z_1 + Z_s)(Z_2 + Z_L)}$	36	2	40	3	0
Z_s, Z_1, Z_3, Z_4	5	$\frac{g_m Z_3 - 1}{1 + Z_s\left(g_m + \frac{1}{Z_1} + \frac{2}{Z_4}\right) + \frac{2Z_3}{Z_4}\left(1 + \frac{Z_s}{Z_1}\right)}$	12	3	15	2	2
Z_s, Z_1, Z_3, Z_5	6	$-\frac{g_m Z_3 Z_5 + Z_3 - Z_5}{g_m Z_s (Z_3 - Z_5) - (Z_3 + Z_5)\left(1 + \frac{Z_s}{Z_1}\right) - 4Z_s}$	2	0	0	1	4
Z_s, Z_1, Z_3, Z_L	7	$\frac{g_m Z_3 - 1}{1 + Z_s\left(g_m + \frac{1}{Z_1} + \frac{1}{Z_L}\right) + \frac{Z_3}{Z_L}\left(1 + \frac{Z_s}{Z_1}\right)}$	12	3	15	1	2
Z_s, Z_1, Z_4, Z_5	8	$-\frac{g_m Z_5 + 1}{Z_s\left(g_m - \frac{1}{Z_1} - \frac{2}{Z_4}\right) - \frac{2Z_s}{Z_4}\left(1 + \frac{Z_s}{Z_1}\right) - 1}$	12	3	14	2	2
Z_s, Z_1, Z_4, Z_L	9	$\frac{g_m Z_1 Z_4 Z_L}{(Z_1 + Z_s)(Z_4 + 2Z_L)}$	36	4	76	3	0
Z_s, Z_1, Z_5, Z_L	10	$\frac{g_m Z_5 + 1}{1 + Z_s\left(\frac{1}{Z_1} + \frac{1}{Z_L} - g_m\right) + \frac{Z_5}{Z_L}\left(1 + \frac{Z_s}{Z_1}\right)}$	12	3	14	1	2
Z_s, Z_2, Z_3, Z_4	11	$\frac{g_m Z_3 - 1}{1 + Z_s\left(g_m + \frac{2}{Z_4} + \frac{1}{Z_2}\right) + Z_3\left(\frac{1}{Z_2} + \frac{2}{Z_4}\right)}$	8	1	19	2	2
Z_s, Z_2, Z_3, Z_5	12	$-\frac{g_m Z_3 Z_5 + Z_3 - Z_5}{g_m Z_s (Z_3 - Z_5) - (Z_3 + Z_5) - 4Z_s - \frac{1}{Z_2}(Z_3 Z_5 + Z_3 Z_s + Z_5 Z_s)}$	2	0	2	1	4
Z_s, Z_2, Z_3, Z_L	13	$\frac{g_m Z_3 - 1}{1 + Z_s\left(g_m + \frac{1}{Z_L} + \frac{1}{Z_2}\right) + Z_3\left(\frac{1}{Z_2} + \frac{1}{Z_L}\right)}$	8	1	19	1	2
Z_s, Z_2, Z_4, Z_5	14	$-\frac{g_m Z_5 + 1}{Z_s\left(g_m - \frac{1}{Z_2} - \frac{2}{Z_4}\right) - Z_5\left(\frac{1}{Z_2} + \frac{2}{Z_4}\right) - 1}$	8	1	18	2	2
Z_s, Z_2, Z_4, Z_L	15	$\frac{g_m}{\frac{1}{Z_L} + \frac{1}{Z_2} + \frac{2}{Z_4}}$	0	0	37	2	0
Z_s, Z_2, Z_5, Z_L	16	$\frac{g_m Z_5 + 1}{1 + Z_s\left(\frac{1}{Z_2} + \frac{1}{Z_L} - g_m\right) + Z_5\left(\frac{1}{Z_2} + \frac{1}{Z_L}\right)}$	8	1	18	1	2
Z_s, Z_3, Z_4, Z_5	17	$-\frac{g_m Z_3 Z_5 + Z_3 - Z_5}{g_m Z_s (Z_3 - Z_5) - (Z_3 + Z_5) - 4Z_s - \frac{2}{Z_4}(Z_3 Z_5 + Z_3 Z_s + Z_5 Z_s)}$	2	1	5	1	4
Z_s, Z_3, Z_4, Z_L	18	$\frac{g_m Z_3 - 1}{1 + Z_s\left(g_m + \frac{1}{Z_L} + \frac{2}{Z_4}\right) + Z_3\left(\frac{2}{Z_4} + \frac{1}{Z_L}\right)}$	8	3	37	1	2
Z_s, Z_3, Z_5, Z_L	19	$\frac{g_m Z_3 Z_5 + Z_3 - Z_5}{g_m Z_s (Z_5 - Z_3) + Z_3 + Z_5 + 4Z_s + \frac{1}{Z_L}(Z_3 Z_5 + Z_3 Z_s + Z_5 Z_s)}$	2	1	5	0	4
Z_s, Z_4, Z_5, Z_L	20	$\frac{g_m Z_5 + 1}{1 + Z_s\left(\frac{2}{Z_4} + \frac{1}{Z_L} - g_m\right) + Z_5\left(\frac{2}{Z_4} + \frac{1}{Z_L}\right)}$	8	3	35	1	2

gain in this case becomes $\widetilde{K} = -[C_s/(C_s + C_{gs})]$ instead of $K = g_m R_3 - 1$. By contrast HP4 can have complex poles with $Q > 1/2$ and gains greater than one are easily achieved. However, factoring in C_{gs} and C_{gd} from (2c) again changes the transfer function to third-order introducing a high frequency zero at $s_z = (1/C_{gd})(g_m + (1/R_5) - (1/R_3))$ and modifies the high frequency gain to $\widetilde{K} = -[C_s/(C_s + C_{gs})]$.

Examining BP5, which is a low Q filter whose pole frequency is dependent on g_m, it is clear that this filter requires the additional biasing current source I_a. However, even when transistor parasitics are considered, its transfer function remains as a second-order while the parameters ω_o, Q and K change to the values shown in Table V with an additional high frequency zero at $s_z = [(g_m R_3 - 1)/(R_3 C_{gd})]$. In contrast BP6 does not require I_a but proper operation requires that $g_m R_L < 1$. It too (like BP5) cannot have complex poles and remains second-order with ω_o, Q, and K changing to the values shown in Table V when transistor parasitics are considered. Looking at BP7 and contrasting it with BP6, its advantage over BP6 is that it can have complex poles, and there are no restrictions on the product $g_m R_L$. However, like BP6 its pole frequency is dependent of g_m.

In BP8, an interesting *LC* filter is developed. This filter requires dc biasing from the input source and can be thought of as the active version of its passive *RLC* counterpart or as a differential single tuned amplifier. It is one of 37 possible BP filters obtainable from filter #15 of Table III. Transconductance g_m controls its gain while R_2 controls its Q, which can be large. Resistance R_s can be of any value as it does not factor into any of the equations. Factoring parasitics, its transfer function

TABLE IV
SAMPLES OF POSSIBLE FILTERS BASED ON VARIOUS CHOICES OF IMPEDANCES TAKEN FROM TABLES II AND III. INCLUDED ALSO ARE INPUT AND OUTPUT IMPEDANCES AT LFS AND HFS

Z impedances	Filter	K / Q	ω_o / Q_z	$Z_{in}(LF)$ / $Z_{in}(HF)$	$Z_{out}(LF)$ / $Z_{out}(HF)$
$L_s, R_3, R_L//C_L$	LP1	$\frac{(g_m R_3-1)R_L}{R_3+R_L}$	$\sqrt{\frac{\left(1+\frac{R_3}{R_L}\right)}{L_s C_L}}$	$\frac{2(R_3+R_L)}{g_m R_L+1}$	$\frac{2R_3R_L}{R_3+R_L}$
		$\frac{1}{\frac{R_3}{L_s}+\frac{1}{C_L}\left(g_m+\frac{1}{R_L}\right)}\sqrt{\frac{\left(1+\frac{R_3}{R_L}\right)}{L_s C_L}}$	–	∞	0
L_s, C_4, R_5, R_L	LP2	$\frac{g_m R_5+1}{1+\frac{R_5}{R_L}}$	$\sqrt{\frac{1+\frac{R_5}{R_L}}{2C_4L_s}}$	$\frac{2(R_5+R_L)}{1-g_m R_L}$	$\frac{2R_5R_L}{R_5+R_L}$
		$\frac{1}{\frac{2R_5}{L_s}-\frac{g_m}{C_4}+\frac{1}{R_L C_4}}\sqrt{\frac{2\left(1+\frac{R_5}{R_L}\right)}{C_4L_s}}$	–	∞	0
C_s, R_3, L_L	HP3	$g_m R_3-1$	$\frac{1}{\sqrt{C_s L_L}}$	∞	0
		$\frac{\sqrt{\frac{C_s}{L_L}}}{R_3C_s+g_m L_L}$	–	$\frac{2}{g_m}$	$2R_3$
C_s, R_3, R_5, L_L	HP4	$\frac{g_m R_3R_5+R_3-R_5}{R_3+R_5}$	$\frac{1}{\sqrt{C_s L_L}}$	∞	0
		$\frac{\left(1+\frac{R_3}{R_5}\right)\sqrt{\frac{C_s}{L_L}}}{R_3C_s+\frac{4L_L}{R_5}+g_m L_L\left(1-\frac{R_3}{R_5}\right)}$	–	$\frac{2(R_3+R_5)}{4+g_m(R_5-R_3)}$	$\frac{2R_3R_L}{R_3+R_L}$
C_s, R_3, C_4	BP5	$\frac{(g_m R_3-1)C_s}{C_s+2C_4}$	$\sqrt{\frac{g_m}{2R_3C_4C_s}}$	∞	$\frac{2}{g_m}$
		$\frac{\sqrt{2g_m R_3C_sC_4}}{C_s+2C_4}$	–	$2R_3$	0
C_s, C_4, R_5, R_L	BP6	$\frac{g_m R_5+1}{1+\frac{2C_4}{C_s}+\frac{R_5}{R_L}}$	$\sqrt{\frac{1-g_m R_L}{2R_5R_LC_4C_s}}$	∞	$\frac{2R_L}{1-g_m R_L}$
		$\frac{\sqrt{2(1-g_m R_L)(R_5R_LC_4C_s)}}{2R_LC_4+R_5C_s+R_LC_s}$	–	$2R_5$	0
C_s, R_3, C_4, R_L	BP7	$\frac{g_m R_3-1}{1+\frac{2C_4}{C_s}+\frac{R_3}{R_L}}$	$\sqrt{\frac{g_m R_L+1}{2C_4C_sR_3L_L}}$	∞	$\frac{2R_L}{1+g_m R_L}$
		$\frac{\sqrt{\frac{2(g_m R_L+1)}{C_4C_sR_3L_L}}}{\frac{2}{R_3C_s}+\frac{1}{R_LC_4}+\frac{1}{R_3C_4}}$	–	$2R_3$	0
R_2, C_4, L_L $Z_s=R_s=0$	BP8	$g_m R_2$	$\sqrt{\frac{1}{2C_4L_L}}$	∞	0
		$R_2\sqrt{\frac{2C_4}{L_L}}$	–	∞	0
R_s, L_4, R_5, C_L	BP9	$\frac{1+g_m R_5}{1-g_m R_s}$	$\sqrt{\frac{1}{2L_4C_L}}$	$2\left(R_5+R_s\right)$	0
		$\frac{(R_5+R_s)\sqrt{\frac{2C_L}{L_4}}}{1-g_m R_s}$	–	$2\left(R_5+R_s\right)$	0
R_s, L_4+C_4, R_5, R_L	BS10	$\frac{1+g_m R_5}{1+\frac{(R_5+R_s)}{R_L}-g_m R_s}$	$\sqrt{\frac{1}{2L_4C_4}}$	$\frac{2(R_s+R_L+R_5-g_m R_sR_L)}{1-g_m R_L}$	$\frac{2(R_5+R_s)R_L}{(R_s+R_L+R_5-g_m R_sR_L)}$
		$\frac{\left(1+\frac{(R_5+R_s)}{R_L}-g_m R_s\right)\sqrt{\frac{L_4}{C_4}}}{R_5+R_s}$	–	$\frac{2(R_s+R_L+R_5-g_m R_sR_L)}{1-g_m R_L}$	$\frac{2(R_5+R_s)R_L}{(R_s+R_L+R_5-g_m R_sR_L)}$
R_s, L_3+C_3, R_5, R_L	GE11	$\frac{R_L(g_m R_5+1)}{R_s+R_5+R_L-g_m R_sR_L}$	$\sqrt{\frac{1}{C_3L_3}}$	$\frac{2(R_s+R_L+R_5-g_m R_sR_L)}{1-g_m R_L}$	$\frac{2(R_5+R_s)R_L}{(R_s+R_L+R_5-g_m R_sR_L)}$
		$\frac{R_5+R_L+R_s(1-g_m R_L)}{R_5(R_s+R_L)+4R_sR_L+g_m R_sR_5R_L}\sqrt{\frac{L_3}{C_3}}$	$-\frac{g_m R_5+1}{R_5}\sqrt{\frac{L_3}{C_3}}$	$\frac{2(R_s+R_L+R_5-g_m R_sR_L)}{1-g_m R_L}$	$\frac{2(R_5+R_s)R_L}{(R_s+R_L+R_5-g_m R_sR_L)}$

changes to third-order with an unwanted high frequency zero at $s_z = (g_m/C_{gd})$. In BP9, a variant of BP8 is presented. Although the load impedance is a capacitor C_L, it does not require the bias current source I_a because dc biasing can be achieved through the inputs. For this circuit to function correctly, $g_m R_s < 1$ must be satisfied. Including parasitics its transfer function changes to third-order with an unwanted high frequency zero at $s_z = (g_m/C_{gd})$.

In BS10, a BS filter capable of generating gains greater than or less than one is presented and its pole and zero frequencies are set by L_4 and C_4. Factoring transmission matrix (2c) reveals however that its transfer function changes to fourth-order with an extra zero at $s_z = [(g_m R_5 + 1)/(R_5 C_{gd})]$. Penultimately in GE11, an interesting GE is presented. Like the previous BS filter, its pole and zero frequency are set by a series combination of L_3 and C_3, as given in Table IV.

TABLE V
EFFECT OF C_{gs}, C_{gd}, AND r_o ON K, Q AND ω_o FOR BP FILTERS BP5, BP6, AND BP7 IN TABLE V. NOTE THAT EACH FILTER REMAINS SECOND-ORDER UNLIKE BP8 AND BP9

Filter	$\widetilde{K}$	$\widetilde{\omega}_o$
	$\widetilde{Q}$	–
BP5	$\frac{(g_m R_3-1)C_s}{2C_4+R_3C_{gd}\left(g_m+\frac{1}{r_o}\right)+(C_{gs}+C_s)\left(1+\frac{R_3}{r_o}\right)}$	$\sqrt{\frac{(g_m r_o+1)/R_3 r_o}{2C_4(C_{gd}+C_{gs}+C_s)+C_{gd}(C_s+C_{gs})}}$
	$\frac{\sqrt{(g_m r_o+1)R_3 r_o\left(2C_4(C_{gd}+C_{gs}+C_s)+C_{gd}(C_s+C_{gs})\right)}}{(C_{gs}+C_s)(R_3+r_o)+2C_4 r_o+C_{gd}R_3(g_m r_o+1)}$	–
BP6	$\frac{(g_m R_5+1)R_L C_s r_o}{(C_s+C_{gs})(R_5R_L+R_5r_o+R_L r_o)+2C_4R_L r_o+C_{gd}(R_5R_L+R_5r_o+4R_L r_o+R_5R_L g_m r_o)}$	$\sqrt{\frac{(r_o+R_L-g_m R_L r_o)/R_5R_L r_o}{2C_4(C_s+C_{gd}+C_{gs})+C_{gd}(C_s+C_{gd})}}$
	$\frac{\sqrt{\left(2C_4(C_s+C_{gd}+C_{gs})+C_{gd}(C_s+C_{gd})\right)}(R_5R_L r_o)(r_o+R_L-g_m R_L r_o)}{(C_s+C_{gs})(R_5R_L+R_5r_o+R_L r_o)+2C_4R_L r_o+C_{gd}(R_5R_L+R_5r_o+4R_L r_o+R_5R_L g_m r_o)}$	–
BP7	$\frac{(g_m R_3-1)R_L C_s r_o}{(C_s+C_{gs})(R_3R_L+R_3r_o+R_L r_o)+2C_4R_L r_o+C_{gd}(R_3R_L+R_3r_o+R_L R_3 g_m r_o)}$	$\sqrt{\frac{[g_m+1/(R_L//r_o)]/R_3}{2C_4(C_s+C_{gd}+C_{gs})+C_{gd}(C_s+C_{gd})}}$
	$\frac{\sqrt{(g_m R_L r_o+R_L+r_o)(R_L R_3 r_o)\left(2C_4(C_{gd}+C_{gs}+C_s)+C_{gd}(C_s+C_{gs})\right)}}{(C_s+C_{gs})(R_3R_L+R_3r_o+R_L r_o)+2C_4R_L r_o+C_{gd}(R_3R_L+R_3r_o+R_L R_3 g_m r_o)}$	–

However, it is capable of generating an allpass filter if one chooses

$$R_s = \frac{(1 - g_m R_L)}{g_m(1 + g_m R_L) + \frac{R_L}{R_5^2}(4 + 6g_m R_5)} \tag{9}$$

subject to $g_m R_L < 1$ which results in $Q_z = -Q = (g_m + (1/R_5))\sqrt{L_3/C_3}$. The gain of this filter is given by

$$K = \frac{R_L}{(R_5 + 2R_L)} \frac{\left(g_m R_5^2(1 + g_m R_L) + R_L(4 + 6g_m R_5)\right)}{(R_5 + 2R_L + g_m R_5 R_L)}. \tag{10}$$

It is worth mentioning that optimization routines such as *maximize* in Maple can be used to determine Q limits and element spread in potential filters. For example, for filter #7 of Table III having $Z_s = 1/sC_s$, $Z_1 = 1/sC_1$, $Z_3 = R_3$, and $Z_L = R_L//C_L$ an RC BP filter results with $Q = [(\sqrt{(1 + g_m R_L)(C_1 + C_s)R_3 R_L C_L})/((C_1+C_s)(R_3+R_L)+ R_L C_L)]$. While this filter is capable of generating $Q > 1/2$, the optimization routine *maximize* reports, $Q_{\max} = 1.52$ at $K_{\max} = 0.77$ which occurs when $C_1 = 4.34C_s$, $C_L = 5.88C_s$, $R_L = 10R_3$, and $g_m = 10/R_3$. If however, $Z_1 = \infty$ (filter #12, Table II), $Q_{\max} = 1.52$ at $K_{\max} = 4.1$ when $C_L = 1.1C_s$, $R_L = 10R_3$, and $g_m = 10/R_3$. Comparing the two filters, while considered low Q filters, the latter is preferable because it can have larger gains with lower spread of capacitance values and one less component.

Finally, it should be noted that symbolic analysis can also be used to study the effect of transistor mismatch. To demonstrate this and using (2a), let us assume that the two-transistors have different transmission matrices $[T_{a,b}]$, such that $a_{12} = -1/g_m$ and $b_{12} = -1/g_m(1 - \epsilon)$ where ϵ represents a mismatch error in g_m of one of the transistors. The remaining transmission matrix elements are for simplicity assumed to remain unchanged; i.e., $a_{11} = b_{11} = 0$, $a_{21} = b_{21} = 0$, and $a_{22} = b_{22} = 0$. Then examining sample filter #2 of Table III, we find that its transfer function changes to

$$H(s) = \frac{Z_1 Z_2 Z_4 g_m\left(1 - \frac{\epsilon}{2}\right)}{(Z_1 + Z_s)(2Z_2 + Z_4)} \tag{11}$$

which reverts back to the result in Table III when $\epsilon = 0$ as expected. From (11) we can safely conclude that the effective $g_{m_{\text{eff}}}$ of this filter is reduced by the factor $g_m(1 - (\epsilon/2))$ due to mismatch. This however is dependent on the filter type. For example in BP6 (see Table IV) we find a change in pole frequency to

$$\omega_o = \sqrt{\frac{1 - g_{m_{\text{eff}}} R_L}{2R_5 R_L C_4 C_s}} \tag{12}$$

where $g_{m_{\text{eff}}} = (2(\epsilon - 1)/\epsilon - 2)g_m$. Ultimately, more insight into deviations in circuit performance due to mismatch can be examined on a case by case basis.

C. Input and Output Impedances

In Table IV, the input and output impedances at low frequency (LF) and high frequency (HF) are given for all sample filters. Several observations can be made.

1) Some filters can have an input and/or output impedance that is negative. These filters inevitably employ some form of positive feedback such as LP2, BP6, and BS10. To understand why, we use the case of LP2 where the ideal frequency dependent input and output impedances are respectively given by

$$Z_{\text{in}}(s) = \frac{2L_s s^2 + \left[2R_5 + \frac{L_s(1 - g_m R_L)}{R_L C_4}\right]s + \frac{R_5 + R_L}{R_L C_4}}{s + \frac{(1 - g_m R_L)}{2R_L C_4}} \tag{13}$$

and

$$Z_{\text{out}}(s) = \frac{\frac{1}{C_4}\left(1 + \frac{R_5}{L_s}\right)s}{s^2 + \left[\frac{R_5}{L_s} + \frac{(1 - g_m R_L)}{2R_L C_4}\right]s + \frac{R_5 + R_L}{2L_s C_4 R_L}}. \tag{14}$$

Clearly, at LF and HF (13) and (14) revert to their respective terms in Table IV. However, for $g_m R_L > 1$, $\Re(Z_{\text{in}}) < 0$ which is undesirable.

2) Some filters are better suited for cascading such as BP8 with its large input impedance and low output impedance

and Z_s is not factored in any of the expressions for ω_o, Q, or K. When considering the finite output resistance of the transistor $Z_{\text{out}}(s)$ is given by

$$Z_{\text{out}}(s) = \frac{s/C_4}{s^2 + \frac{1}{(R_2//r_o)C_4}s + \frac{1}{2C_4L_L}} \tag{15}$$

which peaks at the pole frequency $\omega_o = (1/\sqrt{2C_4L_L})$ to a maximum value of $R_2//r_o$. For HFs and short channel processes however, where (2c) matters, it turns out that both $Z_{\text{in}}(s)$ and $Z_{\text{out}}(s)$ become third-order. While $Z_{\text{out}}(s)$ remains relatively low with a peaking near ω_o, $Z_{\text{in}}(s)$ decreases from ∞ to a low of Z_s. The reason for this is that at very HFs C_{gd} shorts the gate to the drain. Hence, this filter for high frequency applications performs best with a finite R_s, which still allows biasing.

D. Noise

To further quantify and differentiate various filters, noise analysis can also be conducted using the two-port network approach if one recognizes that to add noise models they must be added external to the two-port network as shown in Fig. 2(b). While a detailed treatment is beyond the scope of this paper because of the sheer number of possible filters, we can consider two examples both taken from Table III of filters #18 and #20. BP filters capable of having $Q > 1/2$ result when $Z_s = R_s$, $Z_3 = R_3$, $Z_4 = 1/sC_4$ and $Z_L = sL_L$ or $Z_s = R_s$, $Z_5 = R_5$, $Z_4 = 1/sC_4$ and $Z_L = sL_L$ each from filters #18 and #20, respectively. In both cases the difference between the two BP filters reduces to using R_3 or R_5 since $Z_{s,4,L}$ remains the same. Let us assume for simplicity that for the frequencies of interest we can neglect flicker noise and consider only the dominant thermal noise in identical MOS transistors $M_{a,b}$ drain channel with spectral density of $S_i = 4kT\gamma g_m$ with $\gamma = (2/3)$ [28]. Resistors $R_{s,3,5}$ contribute the standard noise voltage with spectral density of $S_v = 4kTR_{s,3,5}$. Using (2a) and modifying (3a)–(3i) to add the noise models it can be shown that the noise factors of these two BP filters are given by

$$\text{NF}_{R_3} = \left(1 + \frac{R_3}{R_s}\right)\frac{\left(R_s g_m^2 + \frac{2}{3}g_m\right)R_3 + \frac{2}{3}g_m R_s + 1}{(g_m R_3 - 1)^2} \tag{16}$$

and

$$\text{NF}_{R_5} = \left(1 + \frac{R_5}{R_s}\right)\frac{\left(R_s g_m^2 + \frac{2}{3}g_m\right)R_5 + \frac{2}{3}g_m R_s + 1}{(1 + g_m R_5)^2}. \tag{17}$$

Assuming equal R_s, g_m then for $R_3 = R_5$, it follows that $\text{NF}|_{Z_3=R_3} > \text{NF}|_{Z_5=R_5}$ because of the denominator term in (16). Note that the above results are also valid for BP filters designed with $Z_s = R_s$, $Z_4 = sL_4$, $Z_L = 1/sC_L$ and $Z_3 = R_3$ or $Z_5 = R_5$.

III. Experimental Results

To verify the validity of the found filters, five of them were constructed using discrete BS170 MOS transistors. Unless otherwise indicated $V_{\text{dd}} = 5$ V.

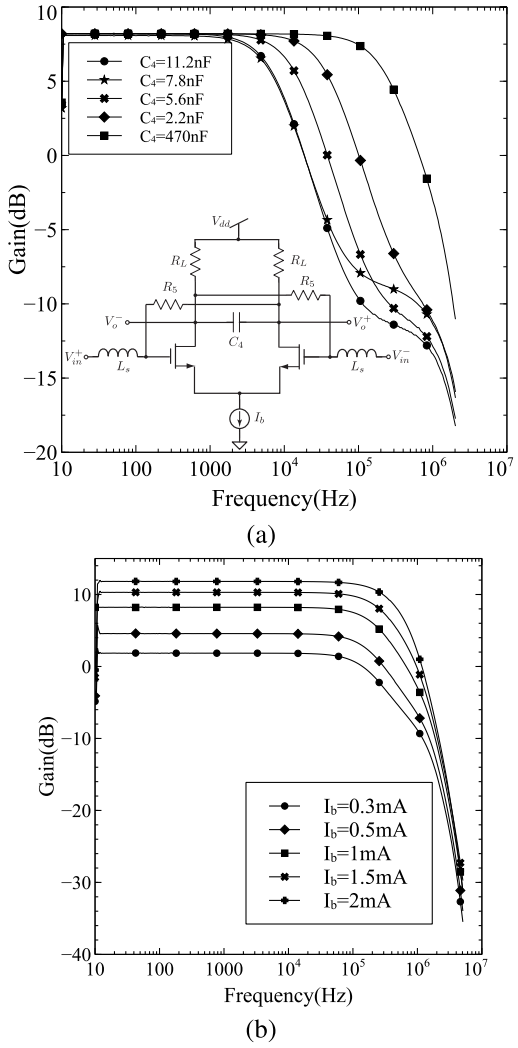

Fig. 4. (a) Measured experimental results for test circuit #1-LP filter with $R_5 = R_L = 2$ kΩ, $L_s = 150$ μH, $I_b = 1$ mA, and C_4 varying to 11.2 nF, 7.8 nF, 5.6 nF, 2.2 nF, and 470 pF. (b) Same circuit but with $C_4 = 470$ pF and I_b varying to values of 0.3 mA, 0.5 mA, 1 mA, and 1.5 mA.

A. Test Circuit #1-Lowpass Filter

In a first test, filter #20 of Table III having $Z_s = sL_s$, $Z_4 = 1/sC_4$, $Z_5 = R_5$, and $Z_L = R_L$ was constructed.

For this impedance combination, an LP filter with

$$K = \frac{g_m R_5 + 1}{1 + \frac{R_5}{R_L}}, \omega_o = \sqrt{\frac{1 + \frac{R_5}{R_L}}{2C_4L_s}}, Q = \frac{\sqrt{\frac{2\left(1+\frac{R_5}{R_L}\right)}{C_4L_s}}}{\frac{2R_5}{L_s} - \frac{g_m}{C_4} + \frac{1}{R_L C_4}} \tag{18}$$

results. The component values used were $R_5 = R_L = 2$ kΩ, $L_s = 150$ μH, and a differential input signal of 20 mV was applied to this circuit. In one experiment with I_b fixed at 1 mA, C_4 was varied using the values of 2.2, 5.6, 7.8, 11.2 nF, and 470 pF, respectively. The results are shown in Fig. 4(a) and indicate a fixed gain of about 9 dB, but as expected changing pole frequency with changing C_4. In Fig. 4(b), C_4 was fixed at 470 pF and I_b varied from 0.5 mA to 3 mA. The dc gain can be observed to change with changing g_m while Q cannot be observed to change because it is low. Finally, for this filter

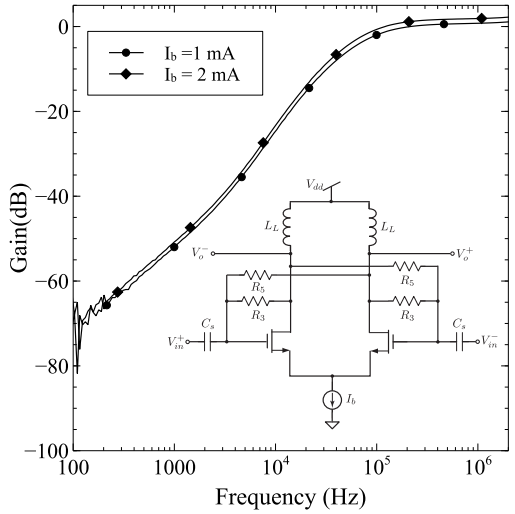

Fig. 5. Measured experimental results for test circuit #2-HP filter having $L_L = 150$ μH, $C_4 = 2.2$ nF, $R_3 = 1$ kΩ, $R_5 = 100$ Ω, and $I_b = 1$ mA and 2 mA.

in terms of impedances $Z_{\text{in}}(\text{LF}) = [(2(R_5 + R_L))/(1 - g_m R_L)]$, $Z_{\text{in}}(\text{HF}) = \infty$ whereas $Z_{\text{out}}(\text{LF}) = [(2R_5 R_L)/(R_5 + R_L)]$, and $Z_{\text{out}}(\text{LF}) = 0$.

B. Test Circuit #2-Highpass Filter

In a second test, filter #19 of Table III having $Z_s = 1/sC_s$, $Z_3 = R_3$, $Z_5 = R_5$, and $Z_L = sL_L$ was constructed. This HP filter has $K = [(g_m R_3 R_5 + R_3 - R_5)/(R_3 + R_5)]$, $\omega_o = [1/(\sqrt{2L_L C_L})]$ and

$$Q = \frac{\left(1 + \frac{R_3}{R_5}\right)\sqrt{\frac{C_s}{L_L}}}{R_3 C_s + \frac{4L_L}{R_5} + g_m L_L\left(1 - \frac{R_3}{R_5}\right)}. \tag{19}$$

The component values used were $L_L = 150$ μH, $C_4 = 2.2$ nF, $R_3 = 1$ kΩ, and $R_5 = 100$ Ω with applied differential input amplitude set at 100 mVpp. The results shown in Fig. 5 for $I_b = 1$ mA and $I_b = 2$ mA indicate a modest change in the high frequency gain which was greater than 0 dB with changing g_m by increasing I_b. For this filter, $Z_{\text{in}}(\text{LF}) = \infty$ decreasing to $Z_{\text{in}}(\text{HF}) = [(2(R_3 + R_5))/(4 + g_m(R_5 - R_3))]$ while $Z_{\text{out}}(\text{LF}) = 0$ increasing to $Z_{\text{out}}(\text{HF}) = [(2R_3 R_5)/(R_3 + R_5)]$.

C. Test Circuit #3-Bandpass Filter

The four-impedance filter #13 taken from Table III having $Z_s = (1/sC_s)$, $Z_2 = (1/sC_2)$, $Z_3 = R_3$, and $Z_L = R_L$ was also constructed and supplied with 9 V. The differential input was set at 20 mV. For this configuration $K = [(g_m R_3 - 1)/(1 + (C_2/C_s) + (R_3/R_L))]$ and

$$\omega_o = \sqrt{\frac{g_m R_L + 1}{R_3 R_L C_2 C_s}},\ Q = \frac{\sqrt{(g_m R_L + 1)(R_3 R_L C_2 C_s)}}{R_L C_2 + R_3 C_3 + R_L C_s}. \tag{20}$$

The fixed component values used were $R_3 = R_L = 2$ kΩ. In a first test, $C_s = C_2$ was varied between the values of 5.6, 2.2 nF, and 470 pF with $I_b = 3$ mA. Varying $C_s = C_2$ as can be expected results in changing pole

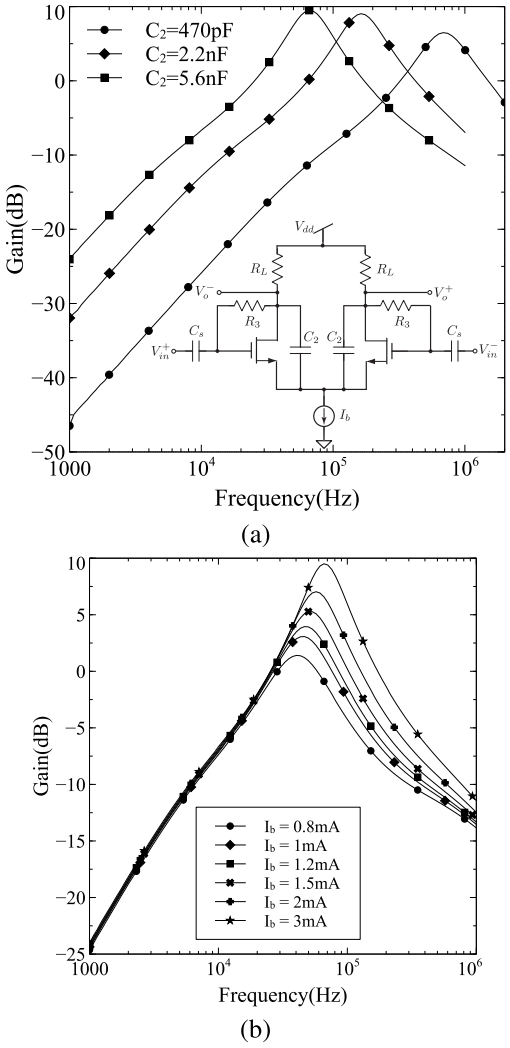

Fig. 6. (a) Measured experimental results for test circuit #3-BP filter having $I_b = 3$ mA, $R_3 = R_L = 2$ kΩ, $C_s = C_2$ with $C_2 = 5.6$ nF, 2.2 nF, and 470 pF. (b) Measured results for the same circuit having $R_3 = R_L = 2$ kΩ, $C_s = C_2 = 5.6$ nF and varying I_b to values of 0.8 mA, 1 mA, 1.2 mA, 2 mA, and 3 mA.

frequency ω_o and Q while keeping K_{BP} constant. The measured results, shown in Fig. 6(a), indicate an increase in center frequency with decreasing capacitance, with $(f_o, Q) = (65.86\ \text{kHz}, 1.33), (163.2\ \text{kHz}, 1.3), (684.5\ \text{kHz}, 1.1)$. The center frequency gain while nearly remaining constant decreases, but can be attributed to changes in component tolerances. In a second test shown in Fig. 6(b), $C_s = C_2 = 5.6$ nF and g_m was varied by changing I_b from 0.8 to 3 mA. In this case the center frequency, Q and center frequency gain can all be easily observed to increase with increasing g_m. Measured results indicate $(f_o, Q) = (40.4\ \text{kHz}, 0.82), (46\ \text{kHz}, 0.95), (47\ \text{kHz}, 0.96), (49.82\ \text{kHz}, 1.02), (57.3\ \text{kHz}, 1.2)$, and $(65.86\ \text{kHz}, 1.33)$. Note if the transmission matrix of (2c) is used instead of (2a), it can be observed that while remaining second order, a zero at $s_z = [(g_m R_3 - 1)/(R_3 C_{gd})]$ exists. It can be observed particularly in Fig. 6(b) for small values of I_b, that is when g_m is small. For this filter, $Z_{\text{in}}(\text{LF}) = \infty$ decreasing to $Z_{\text{in}}(\text{HF}) = 2R_3$ while $Z_{\text{out}}(\text{LF}) = (2R_L/1 + g_m R_L)$ decreasing to $Z_{\text{out}}(\text{HF}) = 0$.

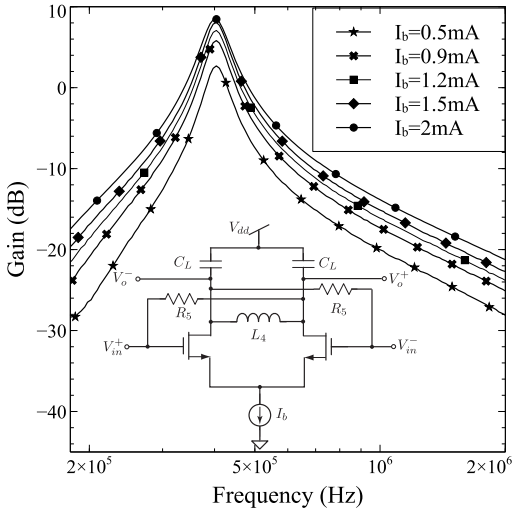

Fig. 7. Measured experimental results for test circuit #5-BP filter having $R_s = 0$, $L_4 = 150$ μH, $C_L = 2.2$ nF, $R_5 = 2$ kΩ and I_b varying as 0.5, 0.9, 1.2, 1.5, and 2 mA.

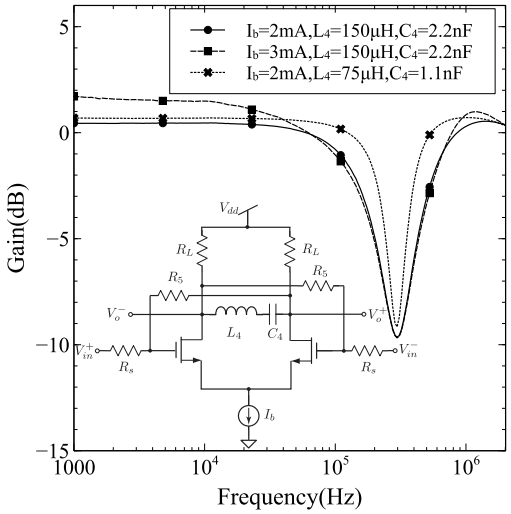

Fig. 8. Measured experimental results for test circuit #6-BS filter to the values given in the inset.

D. Test Circuit #4-Bandpass Filter

In a fourth test, the BP filter arising out of filter #20 of Table III when $Z_s = R_s$, $Z_4 = sL_4$, $Z_5 = R_5$, and $Z_L = 1/sC_L$ was constructed. For this circuit

$$K = \frac{1 + g_m R_5}{1 - g_m R_s}, \omega_o = \sqrt{\frac{2}{L_4 C_L}}, Q = \frac{(R_5 + R_s)\sqrt{\frac{2C_L}{L_4}}}{1 - g_m R_s}. \quad (21)$$

The component values used were $L_4 = 150$ μH, $C_L = 2.2$ nF, $R_5 = 2$ kΩ and the differential input amplitude set at 20 mVpp with offset voltage 2 V on both V_{in}^+ and V_{in}^- for biasing of the transistors. This dc voltage was needed to bias the transistors because $R_s = 0$. Also, no bias current I_a was used. The bias current was initially set at $I_b = 2$ mA and adjusted according to subsequent values of 1.5, 1.2, 0.9, and 0.5 mA. From these values the calculated pole frequency $f_o = 392$ kHz while the measured pole frequency was $f_o = 404$ kHz showing good agreement with the expected results as shown in Fig. 7. The gain can be observed changing from 8.5 dB down to 2.7 dB, with constant $Q = 7.6$ while the pole frequency stayed constant at $f_o = 404$ kHz. For this filter, $Z_{\text{in}}(\text{LF}) = Z_{\text{in}}(\text{HF}) = 2(R_5 + R_s)$ whereas $Z_{\text{out}}(\text{LF}) = Z_{\text{out}}(\text{HF}) = 0$.

E. Test Circuit #5-Bandstop Filter

In a last test, filter #20 of Table III having $Z_s = R_s$, $Z_4 = sL_4 + 1/sC_4$, $Z_5 = R_5$, and $Z_L = R_L$ was constructed. A BS filter results with $K = [(1+g_m R_5)/(1+((R_5+R_s)/R_L)-g_m R_s)]$ and

$$\omega_o = \sqrt{\frac{1}{2L_4 C_4}}, \; Q = \frac{\left(1 + \frac{(R_5+R_s)}{R_L} - g_m R_s\right)\sqrt{\frac{L_4}{C_4}}}{R_5 + R_s}. \quad (22)$$

Three tests were performed with $R_s = R_5 = 100$ Ω and $R_L = 330$ Ω. In the first two tests the inductor and capacitor were fixed as $L_4 = 150$ μH and $C_4 = 2.2$ nF while I_b was varied between 2 and 3 mA. The calculated pole frequency 277 kHz was close to the measured one of 290 kHz and changing I_b only changes Q modestly but a greater change can be observed in the dc gain as shown in Fig. 8. In the third test, the used values were $L_4 = 75$ μH, $C_4 = 1.1$ nF, and $I_b = 2$ mA. The notch frequency and the dc gain should stay the same with a modest change in Q which can be easily observed from Fig. 8.

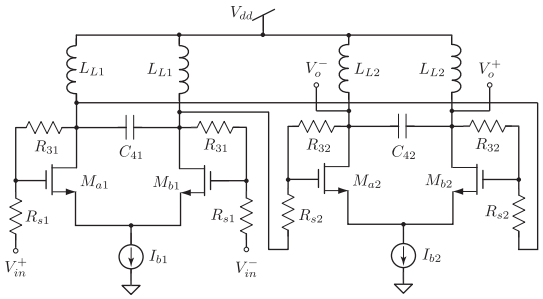

Fig. 9. Fourth-order Chebychev BP filter designed from two cascaded sections of filter #20, taken from Table III.

IV. High Order Filters

Although the automated process based on Maple was restricted to second-order transfer function, higher order differential filters can be obtained by cascading multiple of these second-order sections. To demonstrate this possibility, a fourth-order Chebychev BP with a center frequency of 100 MHz and ripple width of 1 dB was designed using a cascade of two filters, each obtained from filter #20 in Table III with $Z_{si} = R_{si}$, $Z_{3i} = R_{3i}$, $Z_{4i} = 1/sC_{4i}$, and $Z_{Li} = sL_{Li}$ $(i = 1, 2)$. The overall filter is illustrated in Fig. 9 and was simulated in Cadence using a 65-nm CMOS process while powered from a single 1 V supply. Current sources I_{bi} were replaced with transistors M_i with aspect ratios $(W/L)_1 = 3.2$ μm/60 nm, and $(W/L)_2 = 1.2$ μm/60 nm, each biased at 0.55 V which yielded $I_{b1} = 247.2\,\mu$A and $I_{b2} = 90.23\,\mu$A. The aspect ratios of the remaining transistors used were $(W/L)_{a1,b1} = 3.2$ μm/60 nm and $(W/L)_{a2,b2} = 1.2$ μm/60 nm, yielding $g_{m_{a1,b1}} = 2.57$ mA/V and $g_{m_{a2,b2}} = 948.1$ $\mu A/V$, respectively.

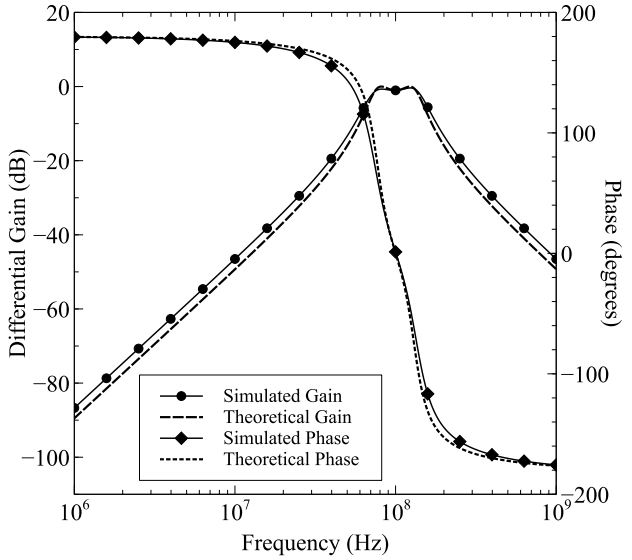

(a)

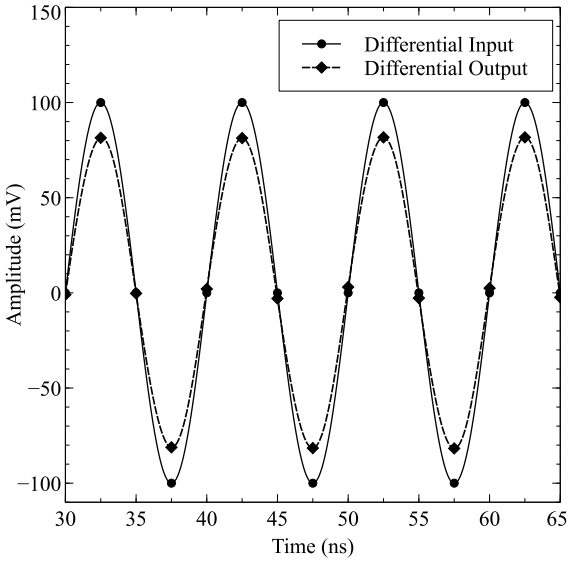

(b)

Fig. 10. (a) Magnitude and phase simulation result along with the theoretical values of the differential forth-order BP filter in Fig. 9. (b) Steady-state time response at the center frequency of 100 MHz. The measured total harmonic distortion (THD) in the output signal is 0.9%.

Component values used for stage 1 were $R_{s1} = 50\ \Omega$, $R_{31} = 5\ \text{k}\Omega$, $C_{41} = 2.14$ pF, and $L_{L1} = 1\ \mu$H. Noting that the output impedance of stage 1, $Z_{\text{out}}(\text{LF}) = Z_{\text{out}}(\text{HF}) \cong 0$ and that it peaks to a value of $[(2(R_{31}+R_{s1}))/((g_{m_{a1,b1}}R_{s1}+1))]$ at that stage pole frequency, the second stage component values were selected as $R_{s2} = 50\ \Omega$, $R_{32} = 2.7\ \text{k}\Omega$, $C_{42} = 0.75$ pF, and $L_{L2} = 1\ \mu$H to reduce loading effect on the first stage. Perfect matching was not achieved, but the simulated results, shown in Fig. 10(a), yielded the desired pole frequency of $f_o = 100$ MHz at a reduced ripple width of 0.55 dB. The steady state time response is shown in Fig. 10(b).

V. Conclusion

In this paper, symbolic CAD analysis was shown to be an extremely powerful tool for filter synthesis.

Algorithm 1 Simple Maple Code to Solve Equations [(3a)–(3i)] Using the *solve* Function in Maple. The Computed Transfer Function $H(s)$ Is the Output

```
# Start of algorithm 1
Eqns := {(3a),(3b),(3c),(3d),(3e),(3f),(3g),(3h),(3i)}:
soln := solve({Eqns,},{Vop,Von,I1a,I2a,V2a,V1a,
V1b,V2b,I1b,I2b,Vin,Vip,Vx}): # Solve for the variables
assign(soln): # Assign the variables
Hs := (Vop-Von)/(Vip-Vin): # Compute the transfer function
Hs := simplify(Hs): # Simplify the transfer function H(s)
# End of algorithm 1
```

Algorithm 2 Maple Code for Computing ω_o, Q, Q_z, K_{LP}, K_{HP}, and K_{BP} From Transfer Function $H(s)$. Input Is the Transfer Function $H(s)$ From the *solve* Function. Output if *temp*=0, Are the Valid Values of ω_o, Q, Q_z, K_{LP}, K_{HP}, and K_{BP}, Else If *temp*=1 All Values Are Invalid Because the Filter Total Order Is Out of Bound

```
# Start of algorithm 2
temp := 0: # Temporary variable acting as a flag.
# Determine the numerator and denominator of H(s)
dn := denom(Hs):nm := numer(Hs):DenOrder := degree(dn,s);
NumOrder := degree(nm,s):TOrder := DenOrder+NumOrder:
# Determine the coefficients of the denominator of H(s)
a := coeff(dn,s,2): b := coeff(dn,s,1): c := coeff(dn,s,0):
  if a=0 or b=0 or c=0 or TOrder>=5 then
     temp := 1 # Setting temp=1 indicates order <> 2nd
  end if;
  if temp=1 then
     a := 1:b := 1:c := 1: # Invalidate any results from this point on
  end if;
# Start of computations for Q, K_LP, K_HP and K_BP constants.
Q := (a/b)*sqrt(c/a,symbolic):Q := simplify(Q,sqrt):
wo_sqr := simplify(c/a): wo := sqrt(wo_sqr);
Bandwidth := (wo/Q): B := collect(Bandwidth,[gm]);
bhp := coeff(nm,s,2): bbp := coeff(nm,s,1): blp := coeff(nm,s,0):
K_LP := simplify(blp/a/wo^2);
K_HP := simplify(bhp/a);
K_BP := simplify(bbp/a/B);
# Compute Q_z if the following conditions are met
   if K_LP=K_HP and K_BP<>0 and K_LP<>0 then
      Qz := simplify(K_LP*Q/K_BP)
   end if;
End of Algorithm 2
```

Remark 1: Comments indicated by #, simplify/collect-Simplify or collect an expression

A differential-input differential-output filter topology based on the basic two-transistor differential-pair structure surrounded by five impedances, a source impedance and load impedance was used in an automated search process using the symbolic capabilities of Maple in order to find all possible transfer

Algorithm 3 Maple Code to Determine the Filter Type From Coefficients K_{LP}, K_{HP}, and K_{BP} of Transfer Function $H(s)$. Inputs Are ω_o, Q, K_{LP}, K_{HP}, K_{BP}, and Empty Matrices of Filter Type_Result. Maintain a Count of Each Filter Type and if Necessary Compute Q_z. Output Filter Type Is Stored in Matrices Indicated by <<>>

```
# Start of Algorithm 3.
# Compute all Highpass filter results
  if temp=0 and K_BP=0 and K_LP=0 then
   HPresult := <HPresult,<Z|wo|Q|K_HP>>:
   CountHP := CountHP+1:
  end if;

# Compute all Bandpass filter results
  if temp=0 and K_HP=0 and K_LP=0 then
   BPresult := <BPresult,<Z|wo|Q|K_BP>>:
   CountBP := CountBP+1:
end if;

# Compute all Lowpass filter results
  if temp=0 and K_HP=0 and K_BP=0 then
   LPresult := <LPresult,<Z|wo|Q|K_LP>>:
   CountLP := CountLP+1:
end if; # Compute all Bandstop filter results

  if temp=0 and K_BP=0 and K_HP<>0 and K_LP<>0 then
   BSresult := <BSresult,<Z|wo|Q|K_HP|K_LP>>:
   CountBS := CountBS+1:
end if;

# Compute all Gain Equalizer filter results
  if temp=0 and K_LP=K_HP and K_BP<>0 and K_LP<>0
then
   Qz := K_LP*Q/K_BP:Qz := simplify(Qz):
   GE_APresult := <GE_APresult,<Z|wo|Q|Qz|K_LP>>:
   CountGE_AP := CountGE_AP+1:
   end if;

# End of Algorithm 3
```

functions and consequently all valid second-order filters from three or four impedance combinations, respectively, satisfying a prespecified set of constraints. A total of 876 filters were found at the end of the search process with their transfer function parameters clearly given symbolically. Sample filters were analyzed to study the effects of the transistor parasitics, noise, and transistor mismatch on the transfer functions. In addition, LP, HP, BP, and BS filters prototypes were designed and experimentally tested. A fourth-order BP filter was also designed and simulated in a 65-nm CMOS process based on one of the discovered second-order filters. It is evident from this paper that the combination of the two-port network circuit modeling approach and symbolic mathematical analysis form a powerful tool that enables the full automation of the search process for valid candidate circuit arising from a certain topology. The derivation of these transfer functions and all corresponding possible filters is otherwise impossible using hand calculation or using any numerical analysis method. It is important to note that transistors or other active building blocks are essentially nonlinear devices while the two-port network modeling assumes a small-signal linear model of the device. However, the two-port network X-parameters, introduced in [29] and [30] particularly for conducting nonlinear analysis can be used to characterize the nonlinear behavior of circuits [31]. The implications of this on the automation process of filters has not yet been explored and is set as a future goal.

APPENDIX

See Algorithms 1–3.

REFERENCES

[1] T. Deliyannis, Y. Sun, and J. K. Fidler, *Continuous Time Active Filter Design*. New York, NY, USA: CRC Press, 1999.

[2] C. Psychalinos, "Low-voltage log-domain complex filters," *IEEE Trans. Circuits Syst. I, Reg. Papers*, vol. 55, no. 11, pp. 3404–3412, Dec. 2008.

[3] A. G. Katsiamis, K. N. Glaros, and E. M. Drakakis, "Insights and advances on the design of CMOS sinh companding filters," *IEEE Trans. Circuits Syst. I, Reg. Papers*, vol. 55, no. 9, pp. 2539–2550, Oct. 2008.

[4] A. Toker, S. Ozoguz, O. Cicekoglu, and C. Acar, "Current-mode all-pass filters using current differencing buffered amplifier and a new high-Q bandpass filter configuration," *IEEE Trans. Circuits Syst. II. Analog Digit. Signal Process.*, vol. 47, no. 9, pp. 949–954, Sep. 2000.

[5] S. A. Mahmoud, M. A. Hashiesh, and A. M. Soliman, "Low-voltage digitally controlled fully differential current conveyor," *IEEE Trans. Circuits Syst. I, Reg. Papers*, vol. 52, no. 10, pp. 2055–2064, Oct. 2005.

[6] A. Abrishamifara, Y. Karimi, and M. M. Navidi, "Current controlled current differential current conveyor: A novel building block for analog signal processing," *IEICE Electron. Express*, vol. 9, no. 2, pp. 104–110, 2012.

[7] K. Entesari and G. M. Rebeiz, "A differential 4-bit 6.5-10-GHz RF MEMS tunable filter," *IEEE Trans. Microw. Theory Techn.*, vol. 53, no. 3, pp. 1103–1110, Mar. 2005.

[8] M. O. Shaker, S. A. Mahmoud, and A. M. Soliman, "New CMOS fully-differential transconductor and application to a fully-differential Gm-C filter," *ETRI J.*, vol. 28, no. 2, pp. 175–181, Apr. 2006.

[9] M. Grashuis, "A fully differential switched capacitor wavelet filter," M.S. thesis, Dept. Microelectron. Comput. Eng., TU Delft, Delft, The Netherlands, Jun. 2009.

[10] X. Meng, W. Li, and G. C. Temes, "A fully-differential input amplifier with band-pass filter for biosensors," in *Proc. IEEE Int. Symp. Circuits Syst. (ISCAS)*, Melbourne, VIC, Australia, 2014, pp. 21–24.

[11] F. Matsumoto, S. Nishioka, T. Ohbuchi, and T. Fujii, "Design of a symmetry-type floating impedance scaling circuits for a fully differential filter," *Analog Integr. Circuits Signal Process.*, vol. 85, no. 2, pp. 253–261, 2015.

[12] A. Ghaffari, E. A. M. Klumperink, and B. Nauta, "A differential 4-path highly linear widely tunable on-chip band-pass filter," in *Proc. IEEE Radio Freq. Integr. Circuits Symp. (RFIC)*, Anaheim, CA, USA, 2010, pp. 299–302.

[13] B. N. Ray, P. P. Chaudhuri, and P. K. Nandi, "Efficient synthesis of OTA network for linear analog functions," *IEEE Trans. Comput.-Aided Design Integr. Circuits Syst.*, vol. 21, no. 5, pp. 517–533, May 2002.

[14] A. Doboli and R. Vemuri, "Exploration-based high-level synthesis of linear analog systems operating at low/medium frequencies," *IEEE Trans. Comput.-Aided Design Integr. Circuits Syst.*, vol. 22, no. 11, pp. 1556–1568, Nov. 2003.

[15] T. McConaghy, P. Palmers, M. Steyaert, and G. G. E. Gielen, "Variation-aware structural synthesis of analog circuits via hierarchical building blocks and structural homotopy," *IEEE Trans. Comput.-Aided Design Integr. Circuits Syst.*, vol. 28, no. 9, pp. 1281–1294, Sep. 2009.

[16] D. Shahhosseini, E. Zailer, L. Behjat, and L. Belostotski, "Method of generating unique elementary circuit topologies," *Can. J. Elect. Comput. Eng.*, vol. 41, no. 3, pp. 118–132, 2018.

[17] H. Tang, H. Zhang, and A. Doboli, "Refinement-based synthesis of continuous-time analog filters through successive domain pruning, plateau search, and adaptive sampling," *IEEE Trans. Comput.-Aided Design Integr. Circuits Syst.*, vol. 25, no. 8, pp. 1421–1440, Aug. 2006.

[18] A. S. Elwakil and B. J. Maundy, "Single transistor active filters: What is possible and what is not," *IEEE Trans. Circuits Syst. I, Reg. Papers*, vol. 61, no. 9, pp. 2517–2524, Sep. 2014.
[19] P. Ahmadi, B. Maundy, A. S. Elwakil, L. Belostotski, and A. Madanayake, "A new second-order all-pass filter in 130-nm CMOS," *IEEE Trans. Circuits Syst. II, Exp. Briefs*, vol. 63, no. 3, pp. 249–253, Mar. 2016.
[20] P. J. Osuch and T. Stander, "A millimeter-wave second-order all-pass delay network in BiCMOS," *IEEE Microw. Wireless Compon. Lett.*, vol. 28, no. 10, pp. 912–914, Oct. 2018.
[21] S. M. Perera *et al.*, "Wideband *N*-beam arrays using low-complexity algorithms and mixed-signal integrated circuits," *IEEE J. Sel. Topics Signal Process.*, vol. 12, no. 2, pp. 368–382, May 2018.
[22] B. J. Maundy, A. S. Elwakil, and S. J. G. Gift, "On a class of cross coupled fully differential filters," *Int. J. Circuit Theory Appl.*, vol. 44, no. 7, pp. 1425–1436, 2016.
[23] B. J. Maundy, A. S. Elwakil, S. Ozoguz, and H. A. Yildiz, "Minimal two-transistor multifunction filter design," *Int. J. Circuit Theory Appl.*, vol. 45, no. 11, pp. 1449–1466, 2017. doi: 10.1002/cta.2319.
[24] *Maple Programming Guide*, Maplesoft, Waterloo, ON, Canada, 2019.
[25] A. S. Elwakil, "Motivating two-port network analysis through elementary and advanced examples," *Int. J. Elect. Eng. Educ.*, vol. 47, no. 4, pp. 404–415, 2010.
[26] H. Du, D. Gorcea, P. P. So, and W. J. Hoefer, "A SPICE analog behavioral model of two-port devices with arbitrary port impedances based on the *S*-parameters extracted from time-domain field responses," *Int. J. Numer. Model. Electron. Netw. Devices Fields*, vol. 21, nos. 1–2, pp. 77–90, 2008.
[27] R. Neumayer, F. Haslinger, A. Stelzer, and R. Weigel, "Synthesis of SPICE-compatible broadband electrical models from n-port scattering parameter data," in *Proc. IEEE Int. Symp. Electromagn. Compat.*, vol. 1. Minneapolis, MN, USA, 2002, pp. 469–474.
[28] B. Razavi, *Design of Analog CMOS Integrated Circuits*, 1st ed. New York, NY, USA: McGraw-Hill, 2001.
[29] D. E. Root, J. Verspecht, J. Horn, and M. Marcu, *X-Parameters: Characterization, Modeling, and Design of Nonlinear RF and Microwave Components* (The Cambridge RF and Microwave Engineering Series), 1st ed. Cambridge, U.K.: Cambridge Univ. Press, 2013.
[30] P. Barmuta, F. Ferranti, A. Lewandowski, L. Knockaert, and D. Schreurs, "Efficient generation of X-parameters transistor models by sequential sampling," *IEEE Microw. Wireless Compon. Lett.*, vol. 24, no. 8, pp. 530–532, Aug. 2014.
[31] R. Essaadali, A. Jarndal, A. B. Kouki, and F. M. Ghannouchi, "On the accurate voltage and current analytical relationship to *X*-parameters of a nonlinear two-port network," *IEEE Trans. Microw. Theory Techn.*, vol. 66, no. 10, pp. 4439–4451, Oct. 2018.